How flexible parasites can outsmart their hosts for evolutionary dominance

Tao Wen [1], Eugene V. Koonin [2], and Kang Hao Cheong [1,*]

[1]*Division of Mathematical Sciences, School of Physical and Mathematical Sciences, Nanyang Technological University, 21 Nanyang Link, S637371, Singapore*

[2]*National Center for Biotechnology Information, National Library of Medicine, National Institutes of Health, Bethesda, Maryland 20894, USA*

(Received 1 June 2023; accepted 31 January 2024; published 30 April 2024)

Antagonistic coevolution between hosts and parasites substantially impacts community structure, with parasites displaying fluctuating selection or arms race dynamics during coevolution. The traditional matching alleles (MA) and gene-for-gene (GFG) models have been used to describe the dynamics and interaction of host-parasite coevolution, with these models assuming that parasites adopt a single strategy when competing with other parasites. We present a nonlinear dynamic population model that challenges this assumption, showing how a parasite that is disadvantaged under either the MA or the GFG model can win the competition by switching between the two losing strategies based on an external environmental cue, internal processes, or stochastic decision-making. This counterintuitive outcome is analogous to Parrondo's paradox, a game-theoretic concept that shows how alternating between two losing strategies can result in a winning outcome. Our numerical experiments support the validity of this model, suggesting that parasites can greatly benefit from maximum flexibility in their interactions with hosts. The flexibility of successful parasites puts an extra burden on the host defenses that have to adapt to different strategies of the parasites. These findings contribute to a deeper understanding of the coevolution of parasites and hosts, with broad implications for the evolution of complex ecological systems.

DOI: 10.1103/PhysRevResearch.6.023104

I. INTRODUCTION

Antagonistic interactions and coevolution between hosts and parasites, as well as competition among parasites, are evolutionary processes that are pervasive in nature and have substantial ecological impacts [1–4]. The dynamics of host-parasite coevolution and competition are highly complex. Anderson and May [5,6] studied the regulatory roles of parasites in host mortality and population growth, respectively. Two types of models capture the fundamental features of these processes. The first model, known as the matching alleles (MA) model, assumes that hosts can defend against any parasites without a matching genotype based on self- versus non-self-discrimination. Under this model infection outcomes depend on the genotypes of both the host and the parasite, resulting in fluctuating selection dynamics and evolution of specialist parasites [7,8]. The MA model has been widely used to study invertebrate immune systems. The second model, known as the gene-for-gene (GFG) model, is widely applied in plant pathology [9,10]. In this model the outcome of an infection is determined by the relationship between the host's resistance loci and the parasite's virulence loci, leading to directional arms race dynamics (ARD) and evolution of generalist parasites [11,12]. These models have been used to solve various key problems in host-parasite coevolution and evolutionary biology [13,14], such as the evolution of sexual reproduction under the red queen hypothesis [15], patterns of local adaptation [16], effects of resistance and virulence [10], tradeoffs found in coevolution between bacteriophages and *Escherichia coli* [17], factors of epidemic dynamics [18], the role of the immunity response [19,20], and evolution of recombination [21].

Recent studies [22,23] still assume that host-parasite coevolution follows either the MA or GFG strategy, meaning that a parasite is either a specialist or generalist. However, Ref. [24] suggested that directional ARD intensifies as the host becomes more exposed to the parasite, which can result in the parasite adopting the GFG (generalist) strategy. Furthermore, the environment can also impact the evolutionary dynamic [12,25,26]. A hybrid MA-GFG model with a single parameter was developed by Agrawal and Lively [9] to describe the host-parasite evolutionary dynamic. This work aims to investigate the effects of parasites switching between specialist and generalist strategies in the hybrid MA-GFG model and how parasites determine their coevolution strategy.

To study the coevolution of hosts and parasites, we develop a population dynamics model describing two distinct parasites competing for the same host. One of the parasites is a specialist, whereas the other one, with inferior traits, can switch between being a specialist or a generalist, under

*kanghao.cheong@ntu.edu.sg

TABLE I. Infection rate γ for different pairs of hosts and parasites. The parameter p determines the interaction between P_2 and H, as well as the position of the parasite on the MA-GFG continuum.

	H_1	H_2
P_1	$f_s(\equiv \gamma_1)$	0
P_2	$pf_g(\equiv \gamma_3)$	$pf_g + (1-p)f_s(\equiv \gamma_4)$

different schemes. Due to its inferior traits (lower burst size, higher mortality, and lower infection rate), the second parasite loses the competition when adopting any of the individual strategies (MA or GFG). However, this disadvantaged parasite can win the competition by switching between the two losing strategies. We also describe three switching schemes that can benefit the disadvantaged parasite, namely, switching (1) in response to an external environment factor, (2) as a result of internal processes, and (3) by stochastic decision-making, which is the most unexpected result. We show that the parasite with inferior traits reaches a higher density in the competition when following each of these switching schemes. This counterintuitive result is analogous to the game-theoretic Parrondo's paradox [27], where switching between two losing strategies can result in a winning outcome. A broad range of real-world biological data is compatible with our conclusions on the advantage of strategy switching by parasites [28,29].

II. MODEL OF HOST-PARASITE COEVOLUTION

The evolution model includes two types of parasites (P_1 and P_2) that infect two types of hosts (H_1 and H_2), with different features. The host has the maximum growth rate α and grows under a logistic growth model determined by the carrying capacity $K = \alpha/\beta$, where β is the competition factor among hosts. The susceptible host can be infected to death by each type of parasite with rate γ, although γ can be equal to 0 in specific cases (Table I). There will be τ copies of the parasite in each infection (burst size τ). The parasites are also inactivated with rate ρ. Hence, the evolution model for the host and parasite is captured by the following differential equations:

$$\begin{aligned}
\dot{H}_1 &= \alpha_1 H_1\left(1 - \frac{H_1}{\alpha_1/\beta_1}\right) - H_1(\gamma_1 P_1 + \gamma_3 P_2),\\
\dot{H}_2 &= \alpha_2 H_2\left(1 - \frac{H_2}{\alpha_2/\beta_2}\right) - \gamma_4 P_2 H_2,\\
\dot{P}_1 &= \gamma_1(\tau_1 - 1)P_1 H_1 - \rho_1 P_1,\\
\dot{P}_2 &= (\tau_2 - 1)P_2(\gamma_3 H_1 + \gamma_4 H_2) - \rho_2 P_2. \qquad (1)
\end{aligned}$$

The initial values, descriptions, and units of parameters incorporated in this evolution model are given in Table II. We employ data from recent host-parasite interaction models and biologically realistic values of the parameters [28,29]. Further details can be found in Appendix A. The infection rate γ varies widely depending on the specific type of infection, related to the value of p (Table I), and the parameter p is used to determine the parasite placement on the MA-GFG continuum [9]. When $p = 0$, the interaction is at the MA end, so that both P_1 and P_2 are specialists that can only infect H_1 or H_2 individually, with the binding affinity f_s. When $p = 1$ the interaction is at the GFG end. In this case, P_1 remains a specialist virus but P_2 is a generalist, which means P_2 can infect both H_1 and H_2. Compared with the specialist host-parasite pair, the binding affinity of the generalist f_g is much lower (around $f_g = 0.1 f_s$). The connection between the two popular models, MA and GFG, is described by linear interpolation and determined by the parameter p. Thus the structure of the host-parasite network changes depending on p [30]. In this model, parasites P_1 and P_2 do not compete directly, but they infect a common host (indirect competition) when $p > 0$.

III. RESULTS

The two types of hosts, H_1 and H_2, have different values of growth rate and competition factor. The parasite P_2 is inferior to P_1 in all respects due to the smaller burst size τ, higher mortality rate ρ, and lower infection rate γ. The infection rate γ determined by parameter p is the key variable in this evolution model because it describes the interaction between hosts and parasites. In particular, P_2 is a pure specialist when $p = 0$ and a pure generalist when $p = 1$. All parameter values

TABLE II. The description, value, and unit of parameters in our proposed evolutionary model. We employ the data from recent host-parasite interaction models and biological realistic values [28,29].

Parameter	Description	Value	Units
H_1, H_2	Host density	$10^3, 10^3$	ml^{-1}
P_1, P_2	Parasite density	$10^6, 10^6$	ml^{-1}
α_1, α_2	Growth rate of host	1,1	h^{-1}
β_1, β_2	Competition factor of host	$10^{-6}, 9\times10^{-6}$	ml/h
τ_1, τ_2	Burst size	50,30	—
ρ_1, ρ_2	Mortality rate of parasite	0.2,0.3	h^{-1}
$\gamma_1, \gamma_3, \gamma_4$	Infection rate	—	ml/h
f_s	Binding affinity for the specialist parasite	10^{-6}	ml/h
f_g	Binding affinity for the generalist parasite	0.9×10^{-7}	ml/h
p	Determining factor	—	—

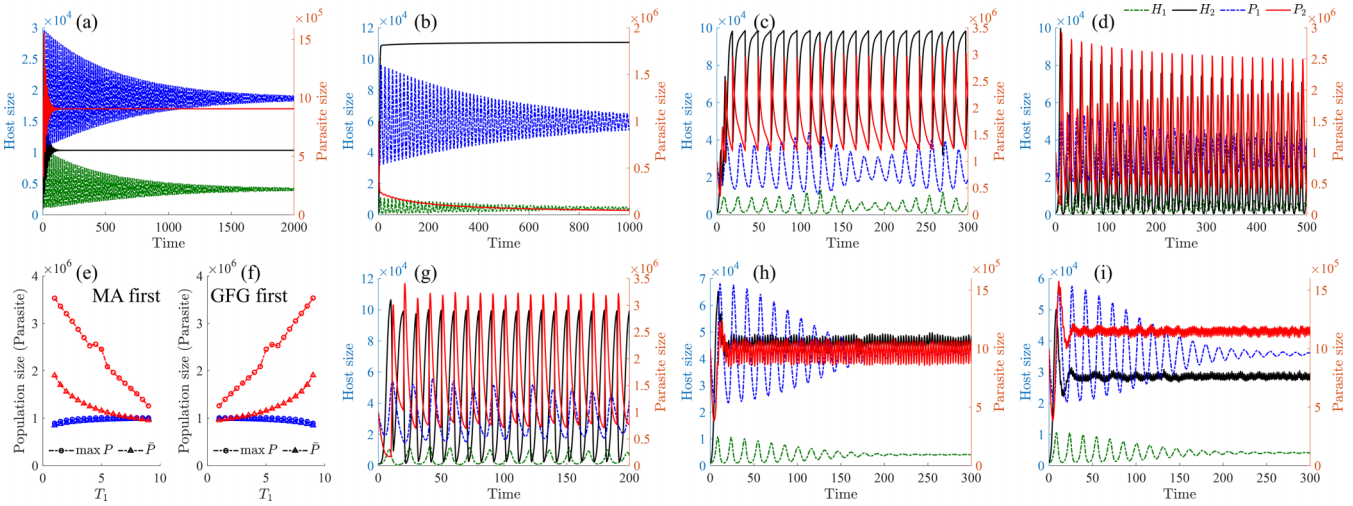

FIG. 1. Population size time series illustrating the competition between parasites under different strategies. Two losing strategies for P_2 result in low density, where P_2 is (a) a specialist (MA end, $p = 0$) or (b) a generalist (GFG end, $p = 1$). The winning outcome for P_2 results from switching schemes based on (c) external environmental condition ($R_U = 72$, $R_L = 12$), (d) periodic internal processes ($T = 10$, $T_1 = 5$), (e) & (f) different orders of the interaction models under the switching scheme based on periodic internal processes ($T_1 \in [1, 9]$, measured in the range [4000, 5000]), (g) quasiperiodic switching scheme ($T = 10$, $T_i \in \{2, 3, 4, 5\}$), (h) stochastic decision-making I ($R = 0.35$, $t_d = 3$, $k = 10^4$), and (i) stochastic decision-making II ($R = 0.5$, $t_d = 2$, $k = 10^4$) individually. All other parameter values are listed in Table II.

are provided in Table II unless stated otherwise. In addition to the average density, typically used to measure species fitness, this work also considers the peak density due to its importance in the competitive dynamics [31–33].

A. Single disadvantage strategy

In the first competition, P_2 adopts a single strategy, that is, either the MA model or the GFG model. Under the MA model [Fig. 1(a)], P_2 undergoes large-amplitude fluctuations in the beginning but stabilizes at around $t = 100$. P_1 also experiences large-amplitude fluctuations that continue for a longer time and then stabilize around $t = 2000$. However, the equilibrium density of P_2 was lower than that of P_1, demonstrating that the specialist strategy is losing for P_2. When P_2 adopts the GFG model [Fig. 1(b)], the evolutionary dynamics of P_1 remain similar to the previous case, with large-scale fluctuations followed by stabilization at around $t = 2000$. In contrast, the density of P_2 experiences a sharp drop and persists at a substantially low density, approaching extinction. Thus, both the pure MA model and the pure GFG model are losing strategies for P_2, as indicated by the lower peak density and average density shown in Table III. The equilibria of each population for different cases are further derived in Appendix B.

B. Switching scheme under external environmental condition—Host exposure to parasite

Biological experiments [24] have shown that increasing host exposure to the parasite (population mixing) promotes both infectivity and resistance, resulting in ARD. There are single alleles that can change the host resistance and parasite host ranges under the GFG model, promoting the evolution of generalists and predisposing the system towards directional ARD [9]. Thus the ratio of the size of the parasite population to the size of the host population can render the parasite to adopt the GFG strategy. In this competition, P_2 could switch between the MA and GFG strategies depending on the relative sizes of the parasite and host population [Fig. 1(c)],

$$p = \begin{cases} 1, & \frac{P_2}{H_1+H_2} > R_U \\ 0, & \frac{P_2}{H_1+H_2} < R_L \end{cases}. \tag{2}$$

When the parasite/host ratio is above R_U, P_2 adopts the GFG model, resulting in directional ARD, and when the ratio is below R_L, P_2 adopts the MA model. In this case both parasites

TABLE III. Average density and peak density of parasites P_1 and P_2 in various scenarios, which are measured in the range [4000, 5000] as the competition entered the steady state by this time. Parameter values are listed in Table II, unless stated otherwise.

Density ($\times 10^6$)	Pure specialist scheme (MA)	Pure generalist scheme (GFG)	External environment condition scheme	Internal periodic scheme	Internal quasiperiodic scheme	Stochastic decision-making scheme I	Stochastic decision-making scheme II
$\bar{P}_1$	0.9959	0.9936	0.8441	0.9644	0.9015	0.9573	0.9553
$\bar{P}_2$	0.9069	0.0263	1.7753	1.1578	1.5609	0.9795	1.1515
max P_1	0.9962	0.9939	1.0354	1.0094	0.9580	0.9628	0.9631
max P_2	0.9069	0.0268	3.0784	2.3855	3.2060	1.0937	1.2065

undergo large-amplitude fluctuations, but P_2 gains advantage over P_1, as indicated by its higher density after $t = 20$. Hence, P_2 succeeds in the competition with a higher peak density and average density (Table III) by alternating its strategy in response to the large population size of H_2. Tradeoffs in the evolutionary dynamics have also been studied under different strategies depending on the host density [34].

C. Switching scheme under internal processes—Biological clock

In the above scenario, the switching strategy employed by the parasite depended on an external environmental factor, namely, the relative densities of the parasite and host populations. We then explored a time-based, periodic switching scheme motivated by the notion of the biological clock, which controls the physiological reactions of organisms, such as feeding behavior, sleep patterns, and hormone release according to the circadian cycle [35–39]. The switching scheme based on internal processes takes the form

$$p = \begin{cases} 0, & 0 < \mathrm{mod}(t, T) \leqslant T_1 \\ 1, & T_1 < \mathrm{mod}(t, T) \leqslant T \end{cases}. \tag{3}$$

Thus, the MA and GFG models are executed sequentially. Specifically, the MA and GFG models are adopted during $(0, T_1]$ and $(T_1, T]$, respectively, and P_2 chooses one of the two models with different values of T_1. Under this scheme [Fig. 1(d)], the fluctuation amplitude of P_2 is greater than that of P_1. However, both the peak density and the average density of P_2 are higher than that of P_1 (Table III), resulting in P_2 winning the competition. Additionally, as the period assigned by the biological clock to a single strategy can vary depending on the species and other factors, the changing value of T_1 has been explored in Fig. 1(e), where peak density and average density are represented by circles and triangles, respectively. The larger the value of T_1, the more time P_2 will allocate to the MA model. The rapidly declining peak density of P_2 is always higher than the slowly rising peak density of P_1, whereas the average density, following the same trend, makes P_2 slightly lower than P_1 when T_1 reaches the maximum value. Thus, the advantage of P_2 weakens as T_1 increases.

The effect of internal processes was further studied [Fig. 1(f)] under different orders of the two strategies (GFG first). In this competition, the GFG and MA strategies are adopted, respectively, during $(0, T_1]$ and $(T_1, T]$,

$$p = \begin{cases} 1, & 0 < \mathrm{mod}(t, T) \leqslant T_1 \\ 0, & T_1 < \mathrm{mod}(t, T) \leqslant T \end{cases}. \tag{4}$$

The advantage of P_2 increases with increasing T_1 as the GFG strategy is adopted first. Similarly, an unexpected win for P_2 is obtained. Overall, in these extreme cases [i.e., $T_1 = 9$ in Fig. 1(e) and $T_1 = 1$ in Fig. 1(f)], P_2 almost exclusively adopts a single losing strategy (the MA model), whereas the alternative strategy (the GFG model) is followed within a very short time frame, which is not enough for P_2 to reverse the outcome and win the competition. Thus, parasites that are originally disadvantaged in the given environment can rely on their internal processes to adjust their switching strategy, finding ways to win in various competitions.

Noise can disrupt the biological clock of an organism, shifting from regular periodic behavior to pseudoregular or even irregular behavior [40,41]. Therefore, a quasiperiodic switching scheme with noise is considered in the competition [Fig. 1(g)], where the MA and GFG models are adopted during $(0, T_i]$ and $(T_i, T]$, respectively:

$$p = \begin{cases} 0, & 0 < \mathrm{mod}(t, T) \leqslant T_i \\ 1, & T_i < \mathrm{mod}(t, T) \leqslant T \end{cases}, \tag{5}$$

where T_i, $i = \lfloor t/T \rfloor$ is a random number selected from a given set that changes in each period i. Even in the presence of noise, the quasiperiodic switching scheme still renders P_2 to win the competition, regardless of the peak density or the average density of the two types of parasites (Table III). This outcome is the same as the periodic switching scheme shown in Fig. 1(d).

D. Switching scheme under stochastic decision-making

Which parasite will win in the competition if P_2 switches between MA and GFG models stochastically, regardless of the external environment factors and the internal state of the parasite? Under stochastic decision-making by P_2, P_2 decides which strategy to adopt every t_d hours,

$$p = \begin{cases} 0, & \mathrm{prob}\, R \\ 1, & \mathrm{prob}\, 1 - R \end{cases}. \tag{6}$$

The MA model is adopted with probability R, and the GFG model is adopted with probability $1 - R$. As this is a random process, the results are recorded over k repetitions. At steady state, the population size of P_2 is greater than that of P_1, that is, P_2 wins the competition [Fig. 1(h) and Table III]. Furthermore, under this random switching scheme, the population of P_2 also stabilizes earlier than the P_1 population. Despite the fact that the density of P_2 is not as high as observed in the previous switching schemes, a winning outcome can still be achieved via stochastic decision-making.

Furthermore, another switching scheme for P_2 under stochastic decision-making was considered, where P_2 directly decides whether to change the previously adopted strategy with probability R every t_d hours,

$$p(t) = \begin{cases} 1 - p(t-1), & \mathrm{prob}\, R \\ p(t-1), & \mathrm{prob}\, 1 - R \end{cases}. \tag{7}$$

In this scheme, P_2 consistently achieves a higher density than P_1 [Fig. 1(i) and Table III]. Compared with the previous scheme under stochastic decision-making, this scheme reduces the fluctuation amplitude of P_2, and its density is consistently higher than that of P_1.

In all competitions (Fig. 1), the interaction between H and P follows the Lotka-Volterra equations [42]. Thus, even when each individual strategy yields a relatively low density of the disadvantaged parasite, alternating between the two losing strategies under each of the three schemes can counterintuitively result in a winning outcome [43], that is, higher density compared to the parasite with superior traits. The case where parasites can adopt $N (N \geqslant 3)$ losing strategies [44] is further explored in Appendix C, and the switching schemes can still

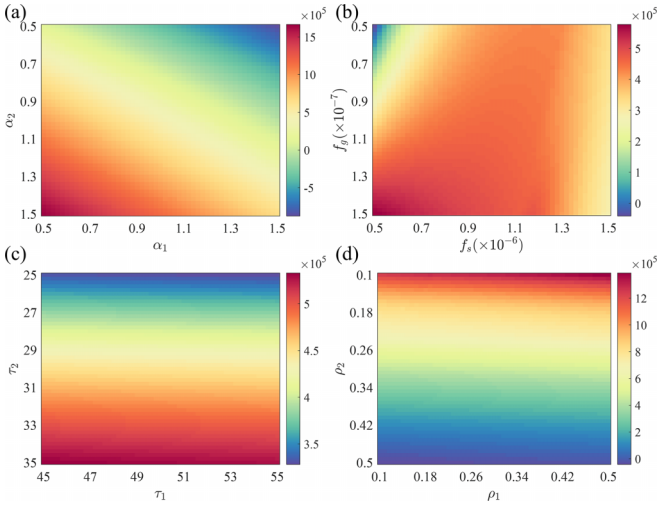

FIG. 2. The parameter space that determines the advantaged parasite in the competition under the switching scheme determined by internal processes. The difference $(P_2 - P_1)$ between the average density of two parasites at $t \in [4000, 5000]$ under the change of (a) growth rate α, (b) binding efficiency f, (c) burst size τ, and (d) mortality rate ρ are shown. Parameter values are listed in Table II unless stated otherwise.

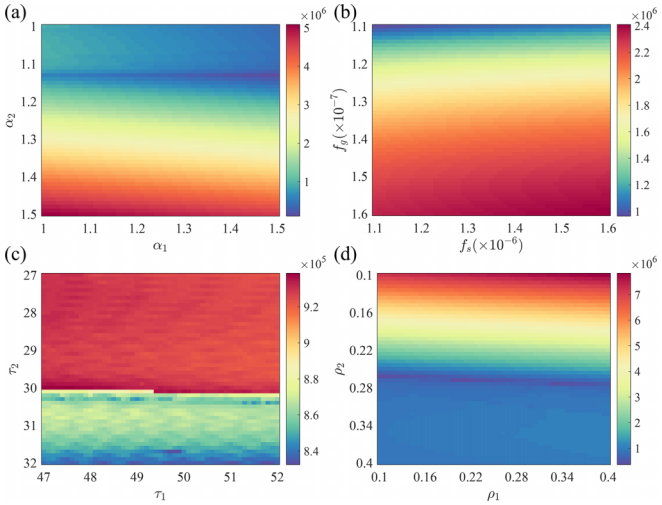

FIG. 3. The parameter space for determining the advantaged parasite under the switching scheme determined by external environmental conditions ($R_U = 72, R_L = 12$). Parameter values are listed in Table II unless stated otherwise.

enable the inferior parasite to win the competition based on peak density.

E. Combinations of parameters yielding Parrondo's paradox

The range of model parameters that determine when P_2 can win the competition due to Parrondo's paradox was further studied by comprehensive simulation, including the parameters that characterize both the host and parasite. The results were evaluated through the difference $(P_2 - P_1)$ between the average densities of the two parasites at $t \in [4000, 5000]$, because the competition entered the steady state by this time. The parameters under the switching scheme based on internal processes ($T = 10, T_1 = 3$) and the external environmental condition ($R_U = 72, R_L = 12$) were analyzed in pairs in Figs. 2 and 3, respectively.

First, the effects of parameters characterizing the hosts [the host growth rate α, Fig. 2(a)] were compared. P_2 wins the competition between the two parasites at higher values of α_2 and lower values of α_1, because only P_2 can get enough resources from H_2 when H_2 grows fast. The effects of H_1 on P_1 and P_2 are similar and are determined by the interaction efficiency. Therefore, the effect of α_2 is more pronounced than that of α_1 under the same scale of changes. Then, the parameters pertaining to parasites themselves were compared. With respect to the interaction affinity for a specialist parasite f_s and a generalist parasite f_g [Fig. 2(b)], P_2 enjoys an advantage in a large range, that is, low values of f_s and high values of f_g. P_2 only loses the competition at low values of f_s and f_g because more resources will be obtained by P_1. The burst size τ_1 of P_1 has no obvious impact on the result, and only τ_2 determines the outcome of the competition [Fig. 2(c)]. The advantage of P_2 is strengthened at higher τ_2, which is consistent with intuitive expectations: features that enable a parasite to survive in the environment give it an advantage. The mortality rates were studied in the interval $\rho_1, \rho_2 \in [0.1, 0.5]$, with P_2 having an advantage across this range [Fig. 2(d)]. At lower ρ_2, the advantage of P_2 is greater, for the same reason as in the case of Fig. 2(c).

Figure 3 explores parameter effects under external condition-driven switching, contrasting with the internal process determinants in Fig. 2. However, P_2 is able to consistently outperform its competitors to win the competition in most of the parameter space. Through comprehensive simulation experimental analysis, the disadvantaged parasite P_2 is able to achieve counterintuitive winning results by switching between losing strategies at different timescales and parameter spaces. This shows that the more flexible a parasite is, the better it fares in evolutionary competitions, even with inferior traits.

IV. DISCUSSION

In this work, we investigated competition between parasites depending on the flexibility of their host interaction strategies. We show that a disadvantaged parasite can outcompete a fitter one by alternating between two losing strategies. Regardless of whether the fitter parasite is a specialist (MA model) or a generalist (GFG model), its density is always lower than that of its competitor, which represents individually losing strategies [Figs. 1(a) and 1(b)]. We show that a disadvantaged parasite can win the competition by alternating strategies under three distinct switching schemes: external environmental condition (host exposure to parasite), internal processes (for example, biological clock), and stochastic (random) decision-making (Fig. 1). This counterintuitive result is analogous to the framework of game theory, in terms of Parrondo's paradox, that is, a winning outcome caused by switching between two losing strategies. Generally, each of the two parasites is envisaged being restricted to its basin of attraction on the fitness landscape due to unpassable valleys of low fitness. However, switching between losing strategies allows the parasite to cross the formerly prohibiting valleys

and reach a region of the landscape corresponding to higher fitness. Similar phenomena appear to be common in multiple biological contexts [45], such as nomadic and colonial lifestyles of animals [43], periodic intercellular competition in multicellular organisms [46] (similar to the maximized population fitness under the competition between a cheater and co-operator [47]), and lytic cycle versus lysogeny in bacteriophages [48].

The parameters that determine the outcome for different types of parasites competing for the same host are poorly understood. We studied the behavior of the model under varying parameter combinations, including features of both the hosts and the parasites, and further explored the parameter space that determines which parasite reaches higher density under switching schemes based on internal processes (Fig. 2) and external environmental conditions (Fig. 3). For the analysis of the model parameters, we employed the data from several biological studies under identical laboratory conditions [28,29]. The results of this analysis reveal the conditions under which the disadvantaged parasite wins the competition by alternating losing strategies, according to Parrondo's paradox.

The general conclusion from this analysis of host-parasite coevolution models is that the more flexible a parasite is in its interactions with the host, the better it fares in evolutionary competitions. Arguably, the flexibility of successful parasites puts an extra burden on the host defenses that have to adapt to different strategies of the parasites.

The code is available at OSF [49].

ACKNOWLEDGMENTS

K.H.C. and T.W. were supported by the Singapore Ministry of Education (MOE) Academic Research Fund (AcRF) Tier 2 Grant No. MOET2EP50120-0021. E.V.K. was supported by the Intramural Research Program of the National Institutes of Health of the USA (National Library of Medicine).

APPENDIX A: PARAMETER VALUES DETERMINATION

The selection process for parameter values in this work is introduced below. In the coevolution model [28], the initial condition for a parasite is set at 10^6 ml^{-1}, while for a host it spans a range from 10^2 to 10^3 ml^{-1}. Hence, the initial parasite and host densities are set to 10^6 and 10^3 ml^{-1}, respectively, in this work. For the host, its growth rate α is simplified to a constant value 1 h^{-1} from the dynamic form [28], which originally ranges from 1 h^{-1} to 1.2 h^{-1}. The competition factor β is determined by the value of $K = \alpha/\beta = 10^6$ ml^{-1} according to [28]. For the parasite, its burst size τ is set to either 30 or 50, falling within the range of [30, 50] as specified in [28]. The mortality rate ρ is chosen to be either 0.2 or 0.3 h^{-1}, approximating the original setting 0.2 h^{-1} in [28]. The binding affinity for the speciality parasite f_s remains consistent with the original setting 10^{-6} ml/h. However, for the generalist parasite, f_s is chosen to be 0.9×10^{-7} ml/h, falling within the range of $[0.01 \times f_s, 0.1 \times f_s] = [0.1 \times 10^{-7}, 10^{-7}]$ [28]. Notably, [28] claims that the utilized parameter values are drawn from biologically realistic values in [29].

APPENDIX B: POPULATION EQUILIBRIUM

The population equilibrium of the model when there is only one parasite is first explored. The first one is that there is only P_1 in the interaction to infect two types of hosts. The equilibrium $x_1^\dagger = (H_1^\dagger, H_2^\dagger, P_1^\dagger, 0)$ of each population can be obtained by setting $\dot{H}_1, \dot{H}_2, \dot{P}_1 = 0$. In this case, the evolutionary model is

$$\begin{aligned} \alpha_1 H_1^\dagger \left(1 - \frac{H_1^\dagger}{\alpha_1/\beta_1}\right) - H_1^\dagger \gamma_1 P_1^\dagger &= 0, \\ \alpha_2 H_2^\dagger \left(1 - \frac{H_2^\dagger}{\alpha_2/\beta_2}\right) &= 0, \\ \gamma_1(\tau_1 - 1) P_1^\dagger H_1^\dagger - \rho_1 P_1^\dagger &= 0. \end{aligned} \tag{B1}$$

Here, $H_2^\dagger$ will reach the environmental carrying capacity $K_2 = \alpha_2/\beta_2$, and $H_1^\dagger = \frac{\rho_1}{\gamma_1(\tau_1 - 1)}$ because $\dot{P}_1 = 0$. Based on the density of hosts, $P_1^\dagger$ can be obtained by $\frac{\alpha_1}{\gamma_1}(1 - \frac{H_1^\dagger}{\alpha_1/\beta_1})$.

The other case is that there is only P_2 in the interaction to infect two types of hosts. The equilibrium $x_2^\circ = (H_1^\circ, H_2^\circ, 0, P_2^\circ)$ of each population can be obtained by setting $\dot{H}_1, \dot{H}_2, \dot{P}_2 = 0$, and the evolutionary model is

$$\begin{aligned} \alpha_1 H_1^\circ \left(1 - \frac{H_1^\circ}{\alpha_1/\beta_1}\right) - \gamma_3 H_1^\circ P_2^\circ &= 0, \\ \alpha_2 H_2^\circ \left(1 - \frac{H_2^\circ}{\alpha_2/\beta_2}\right) - \gamma_4 P_2^\circ H_2^\circ &= 0, \\ (\tau_2 - 1) P_2^\circ (\gamma_3 H_1^\circ + \gamma_4 H_2^\circ) - \rho_2 P_2^\circ &= 0. \end{aligned} \tag{B2}$$

It can be easily obtained that

$$\gamma_3 H_1^\circ + \gamma_4 H_2^\circ = \frac{\rho_2}{(\tau_2 - 1)}. \tag{B3}$$

In addition, H_1° and H_2° can be obtained by

$$H_1^\circ = \left(1 - \frac{\gamma_3 P_2^\circ}{\alpha_1}\right)\alpha_1/\beta_1 \tag{B4}$$

and

$$H_2^\circ = \left(1 - \frac{\gamma_4 P_2^\circ}{\alpha_2}\right)\alpha_2/\beta_2. \tag{B5}$$

By simplifying Eq. (B3) by Eqs. (B4) and (B5), the following formula can be obtained:

$$\gamma_3\left(1 - \frac{\gamma_3 P_2^\circ}{\alpha_1}\right)\alpha_1/\beta_1 + \gamma_4\left(1 - \frac{\gamma_4 P_2^\circ}{\alpha_2}\right)\alpha_2/\beta_2 = \frac{\rho_2}{(\tau_2 - 1)}, \tag{B6}$$

and thus P_2° is expressed by

$$P_2^\circ = \frac{\gamma_3 \frac{\alpha_1}{\beta_1} + \gamma_4 \frac{\alpha_2}{\beta_2} - \frac{\rho_2}{(\tau_2 - 1)}}{\frac{\gamma_3^2}{\beta_1} + \frac{\gamma_4^2}{\beta_2}}. \tag{B7}$$

The expression of H_1° and H_2° can be easily obtained based on Eq. (B7).

The population equilibrium of the model $x_3^\ddagger = (H_1^\ddagger, H_2^\ddagger, P_1^\ddagger, P_2^\ddagger)$ when all populations exist can be obtained by setting $\dot{H}_1, \dot{H}_2, \dot{P}_1, \dot{P}_2 = 0$. The evolutionary model can be obtained,

$$\begin{aligned}
\alpha_1 H_1^\ddagger\left(1-\frac{H_1^\ddagger}{\alpha_1/\beta_1}\right) - H_1^\ddagger(\gamma_1 P_1^\ddagger + \gamma_3 P_2^\ddagger) = 0,\\
\alpha_2 H_2^\ddagger\left(1-\frac{H_2^\ddagger}{\alpha_2/\beta_2}\right) - \gamma_4 P_2^\ddagger H_2^\ddagger = 0,\\
\gamma_1(\tau_1-1)P_1^\ddagger H_1^\ddagger - \rho_1 P_1^\ddagger = 0,\\
(\tau_2-1)P_2^\ddagger(\gamma_3 H_1^\ddagger + \gamma_4 H_2^\ddagger) - \rho_2 P_2^\ddagger = 0. \qquad \text{(B8)}
\end{aligned}$$

Similarly, $H_1^\ddagger$ should be $\frac{\rho_1}{\gamma_1(\tau_1-1)}$ due to $\dot{P}_1 = 0$. Bringing the expression of $H_1^\ddagger$ into $\dot{P}_2 = 0$, $H_2^\ddagger$ can be obtained by

$$H_2^\ddagger = \frac{\rho_2 - \rho_1\frac{(\tau_2-1)\gamma_3}{(\tau_1-1)\gamma_1}}{(\tau_2-1)\gamma_4}. \qquad \text{(B9)}$$

In this case, the expressions of $P_1^\ddagger$ and $P_2^\ddagger$ can be easily obtained,

$$\begin{aligned}
P_2^\ddagger &= \frac{\alpha_2 - \beta_2 H_2^\ddagger}{\gamma_4},\\
P_1^\ddagger &= \frac{\alpha_1 - \beta_1 H_1^\ddagger - \gamma_3 P_2^\ddagger}{\gamma_1}. \qquad \text{(B10)}
\end{aligned}$$

APPENDIX C: SWITCHING SCHEME WITH N LOSING STRATEGIES

The disadvantaged parasite can switch among $N \geqslant 3$ losing strategies in the evolutionary model. The switching scheme based on the external environmental condition (relative sizes of the parasite and host population) is

$$p = \begin{cases} 1, & \frac{P_2}{H_1+H_2} > R_{N-1} \\ i/(N-1), & R_{i+1} > \frac{P_2}{H_1+H_2} > R_i, \\ 0, & \frac{P_2}{H_1+H_2} < R_1 \end{cases} \qquad \text{(C1)}$$

where $i \in \{1, 2, \ldots, N-2\}$ and $\mathbf{R} = [R_1, R_2, \ldots, R_{N-1}]^T$. Apart from $p = 1$ (GFG model) and $p = 0$ (MA model), the value of p can be 0.5 when the relative size of the parasite and host population (host exposure to parasite [24]) is between R_1 and R_{N-1}. This is reasonable because the parasite can adopt more suitable strategies according to the external environmental conditions that they face. Similarly, the switching scheme based on internal processes is

$$p = \begin{cases} 1, & T_{N-1} < \mathrm{mod}(t,T) < T \\ i/(N-1), & T_i < \mathrm{mod}(t,T) < T_{i+1}, \\ 0, & 0 < \mathrm{mod}(t,T) < T_1 \end{cases} \qquad \text{(C2)}$$

where $i \in \{1, 2, \ldots, N-2\}$ and $\mathbf{T} = [T_1, T_2, \ldots, T_{N-1}]^T$.

TABLE IV. Peak density of parasites P_1 and P_2 in different scenarios which are measured in the range [4000, 5000]. Parameter values are listed in Table II, unless stated otherwise.

	Strategy	max $P_1(\times 10^6)$	max $P_2(\times 10^6)$
N=3	$p = 0$	2.0193	0.9069
	$p = 0.5$	1.9340	1.5273
	$p = 1$	2.0158	0.0263
	Internal process	2.3886	3.0323
	External environment condition	1.7690	2.7720
N=6	$p = 0$	3.3871	0.9069
	$p = 0.2$	3.3194	1.0847
	$p = 0.4$	3.1958	1.3434
	$p = 0.6$	3.0344	1.7492
	$p = 0.8$	2.8577	2.4245
	$p = 1$	3.1631	1.0629
	Internal process	3.2113	3.4623
	External environment condition	2.7402	2.7841

The peak density of each parasite in different scenarios is shown in Table IV. When there are $N = 3$ strategies implemented individually (with $\alpha_1 = 2$), the population size of P_2 is consistently smaller than that of P_1 for each strategy individual. The difference between the two parasites is smallest when $p = 0.5$. A similar pattern can be obtained when six losing strategies can be adopted individually (with $\alpha_1 = 3$ and $f_g = 10^{-7}$): the difference is minimized at $p = 0.8$, and the largest difference is observed in the extreme cases (GFG model and MA model). However, under the two switching schemes based on internal process and external environmental conditions, P_2 can win the competition, for both $N = 3$ ($\mathbf{R} = [40, 44]^T$ and $T = 20$, $\mathbf{T} = [5, 10]^T$) and $N = 6$ ($\mathbf{R} = [33, 36, 39, 42, 45]^T$ and $T = 30$, $\mathbf{T} = [5, 8, 14, 20, 27]^T$). The peak density of P_2 substantially surpasses that of P_1 when P_2 switches among three losing strategies. In contrast, the peak density of P_2 is only slightly different from that of P_1 with six losing strategies for P_2, but P_2 still wins the competition. Therefore, both switching schemes with $N \geqslant 3$ losing strategies can allow the disadvantaged parasite to win in the competition when measured by the peak density. Overall, when more losing strategies are involved, the winning advantage of P_2 is weaker. This means that switching schemes can facilitate a slightly disadvantaged population to reverse and win, but when the disadvantage is substantial, the reversal may not occur as expected.

[1] A. G. Clark and L. Pachter, Evolution of genes and genomes on the drosophila phylogeny, Nature (London) **450**, 203 (2007).

[2] S. B. Araujo, M. E. Borges, F. W. von Hartenthal, L. R. Jorge, T. M. Lewinsohn, P. R. Guimarães Jr., and M. van Baalen, Coevolutionary patterns caused by prey selection, J. Theor. Biol. **501**, 110327 (2020).

[3] M. Perc, J. Gómez-Gardenes, A. Szolnoki, L. M. Floría, and Y. Moreno, Evolutionary dynamics of group interactions on

structured populations: A review, J. R. Soc. Interface. **10**, 20120997 (2013).
[4] D. J. Futuyma and M. Slatkin, *Coevolution* (Sinauer Associates, Sunderland, Massachusetts, 1983).
[5] R. M. Anderson and R. M. May, Regulation and stability of host-parasite population interactions: I. Regulatory processes, J. Anim. Ecol. **47**, 219 (1978).
[6] R. M. May and R. M. Anderson, Regulation and stability of host-parasite population interactions: II. Destabilizing processes, J. Anim. Ecol. **47**, 249 (1978).
[7] R. K. Grosberg and M. W. Hart, Mate selection and the evolution of highly polymorphic self/nonself recognition genes, Science **289**, 2111 (2000).
[8] M. Salathé, R. D. Kouyos, and S. Bonhoeffer, The state of affairs in the kingdom of the red queen, Trends Ecol. Evol. **23**, 439 (2008).
[9] A. Agrawal and C. M. Lively, Infection genetics: Gene-for-gene versus matching-alleles models and all points in between, Evol. Ecol. Res. **4**, 91 (2002).
[10] M. A. Parker, Pathogens and sex in plants, Evol. Ecol. **8**, 560 (1994).
[11] J. N. Thompson and J. J. Burdon, Gene-for-gene coevolution between plants and parasites, Nature (London) **360**, 121 (1992).
[12] A. Sasaki, Host-parasite coevolution in a multilocus gene-for-gene system, Proc. R. Soc. London B **267**, 2183 (2000).
[13] S. N. Chowdhury, J. Banerjee, M. Perc, and D. Ghosh, Eco-evolutionary cyclic dominance among predators, prey, and parasites, J. Theor. Biol. **564**, 111446 (2023).
[14] C. Feng, J. Wu, H. Wei, L. Xu, and Q. Zou, CRCF: A method of identifying secretory proteins of malaria parasites, IEEE/ACM Trans. Comput. Biol. Bioinf. **19**, 2149 (2021).
[15] C. M. Lively, A review of red queen models for the persistence of obligate sexual reproduction, J. Hered. **101**, S13 (2010).
[16] S. P. Otto and S. L. Nuismer, Species interactions and the evolution of sex, Science **304**, 1018 (2004).
[17] R. Beardmore, M. Hewlett, R. Peña Miller, I. Gudelj, and J. R. Meyer, Canonical host-pathogen tradeoffs subverted by mutations with dual benefits, Am. Nat. **201**, 659 (2023).
[18] S. Maslov and K. Sneppen, Severe population collapses and species extinctions in multihost epidemic dynamics, Phys. Rev. E **96**, 022412 (2017).
[19] S. Pilosof, S. A. Alcala-Corona, T. Wang, T. Kim, S. Maslov, R. Whitaker, and M. Pascual, The network structure and eco-evolutionary dynamics of CRISPR-induced immune diversification, Nat. Ecol. Evol. **4**, 1650 (2020).
[20] H. Danyun, W. Qian, and L. Wing-Cheong, Mathematical analysis of macrophage-bacteria interaction in tuberculosis infection, Discrete Contin. Dyn. Syst. Ser. B **23**, 3387 (2018).
[21] A. D. Morgan, S. Gandon, and A. Buckling, The effect of migration on local adaptation in a coevolving host–parasite system, Nature (London) **437**, 253 (2005).
[22] S. E. Townsend, S. Newey, S. J. Thirgood, L. Matthews, and D. T. Haydon, Can parasites drive population cycles in mountain hares? Proc. R. Soc. B **276**, 1611 (2009).
[23] J. F. Rabajante, J. M. Tubay, H. Ito, T. Uehara, S. Kakishima, S. Morita, J. Yoshimura, and D. Ebert, Host-parasite red queen dynamics with phase-locked rare genotypes, Sci. Adv. **2**, e1501548 (2016).
[24] P. Gómez, B. Ashby, and A. Buckling, Population mixing promotes arms race host–parasite coevolution, Proc. R. Soc. B **282**, 20142297 (2015).
[25] R. Mostowy and J. Engelstädter, The impact of environmental change on host–parasite coevolutionary dynamics, Proc. R. Soc. B **278**, 2283 (2011).
[26] L. Lopez Pascua, A. R. Hall, A. Best, A. D. Morgan, M. Boots, and A. Buckling, Higher resources decrease fluctuating selection during host–parasite coevolution, Ecol. Lett. **17**, 1380 (2014).
[27] K. H. Cheong, J. M. Koh, and M. C. Jones, Paradoxical survival: Examining the Parrondo effect across biology, BioEssays **41**, 1900027 (2019).
[28] B. J. Quigley, D. García López, A. Buckling, A. J. McKane, and S. P. Brown, The mode of host–parasite interaction shapes coevolutionary dynamics and the fate of host cooperation, Proc. R. Soc. B **279**, 3742 (2012).
[29] M. De Paepe and F. Taddei, Viruses' life history: Towards a mechanistic basis of a trade-off between survival and reproduction among phages, PLoS Biol. **4**, e193 (2006).
[30] C. O. Flores, J. R. Meyer, S. Valverde, L. Farr, and J. S. Weitz, Statistical structure of host–phage interactions, Proc. Natl. Acad. Sci. USA **108**, E288 (2011).
[31] N. M. Waser and L. A. Real, Effective mutualism between sequentially flowering plant species, Nature (London) **281**, 670 (1979).
[32] A. S. Bell, J. C. De. Roode, D. Sim, and A. F. Read, Within-host competition in genetically diverse malaria infections: Parasite virulence and competitive success, Evolution **60**, 1358 (2006).
[33] O. Huitu, K. Norrdahl, and E. Korpimäki, Competition, predation and interspecific synchrony in cyclic small mammal communities, Ecography **27**, 197 (2004).
[34] M. Boots, A. White, A. Best, and R. Bowers, How specificity and epidemiology drive the coevolution of static trait diversity in hosts and parasites, Evolution **68**, 1594 (2014).
[35] T. A. Bargiello, F. R. Jackson, and M. W. Young, Restoration of circadian behavioural rhythms by gene transfer in drosophila, Nature (London) **312**, 752 (1984).
[36] W. A. Zehring, D. A. Wheeler, P. Reddy, R. J. Konopka, C. P. Kyriacou, M. Rosbash, and J. C. Hall, P-element transformation with period locus DNA restores rhythmicity to mutant, arrhythmic drosophila melanogaster, Cell **39**, 369 (1984).
[37] J. L. Price, J. Blau, A. Rothenfluh, M. Abodeely, B. Kloss, and M. W. Young, Double-time is a novel *Drosophila* clock gene that regulates period protein accumulation, Cell **94**, 83 (1998).
[38] P. E. Hardin, J. C. Hall, and M. Rosbash, Feedback of the drosophila period gene product on circadian cycling of its messenger RNA levels, Nature (London) **343**, 536 (1990).
[39] G. Mazzoccoli, M. Vinciguerra, A. Carbone, and A. Relógio, The circadian clock, the immune system, and viral infections: the intricate relationship between biological time and host-virus interaction, Pathogens **9**, 83 (2020).
[40] W. Pittayakanchit, Z. Lu, J. Chew, M. J. Rust, and A. Murugan, Biophysical clocks face a trade-off between internal and external noise resistance, Elife **7**, e37624 (2018).
[41] F. Beck, B. Blasius, U. Lüttage, R. Neff, and U. Rascher, Stochastic noise interferes coherently with a model biological

clock and produces specific dynamic behaviour, Proc. R. Soc. London B **268**, 1307 (2001).

[42] J. Roughgarden, *Theory of Population Genetics and Evolutionary Ecology: An Introduction* (MacMillan, 1979).

[43] Z. X. Tan and K. H. Cheong, Nomadic-colonial life strategies enable paradoxical survival and growth despite habitat destruction, Elife **6**, e21673 (2017).

[44] Y. Song, C. S. Gokhale, A. Papkou, H. Schulenburg, and A. Traulsen, Host-parasite coevolution in populations of constant and variable size, BMC Evolut. Biol. **15**, 212 (2015).

[45] A. Hastings, Transients: the key to long-term ecological understanding? Trends Ecol. Evol. **19**, 39 (2004).

[46] T. Wen, K. H. Cheong, J. W. Lai, J. M. Koh, and E. V. Koonin, Extending the lifespan of multicellular organisms via periodic and stochastic intercellular competition, Phys. Rev. Lett. **128**, 218101 (2022).

[47] R. C. MacLean, A. Fuentes-Hernandez, D. Greig, L. D. Hurst, and I. Gudelj, A mixture of "cheats" and "co-operators" can enable maximal group benefit, PLoS Biol. **8**, e1000486 (2010).

[48] K. H. Cheong, T. Wen, S. Benler, J. M. Koh, and E. V. Koonin, Alternating lysis and lysogeny is a winning strategy in bacteriophages due to Parrondo's paradox, Proc. Natl. Acad. Sci. USA **119**, e2115145119 (2022).

[49] OSF, https://osf.io/ta9gb/?view_only=f65e198bb7d54f9794e4bde1a09f2c2f.